Standard Reference Materials:

SRM 768: TEMPERATURE REFERENCE STANDARD FOR USE BELOW 0.5 K

R. J. Soulen, Jr.,

and

R. B. Dove

Center for Absolute Physical Quantities
National Measurement Laboratory
National Bureau of Standards
Washington, D.C. 20234

U.S. DEPARTMENT OF COMMERCE, Juanita M. Kreps, Secretary

Jordan J. Baruch, Assistant Secretary for Science and Technology

NATIONAL BUREAU OF STANDARDS, Ernest Ambler, Director

Issued April 1979

Library of Congress Catalog Card Number: 79-600014

National Bureau of Standards Special Publication 260-62
Nat. Bur. Stand. (U.S.), Spec. Publ. 260-62, 47 pages (Apr. 1979)
CODEN: XNBSAV

U.S. GOVERNMENT PRINTING OFFICE
WASHINGTON: 1979

For sale by the Superintendent of Documents, U.S. Government Printing Office, Washington, D.C. 20402
Stock No. 003-003-02047-8 Price $2.30
(Add 25 percent additional for other than U.S. mailing).

☆ U.S. GOVERNMENT PRINTING OFFICE: 1979 O—281-069 (85)

PREFACE

Standard Reference Materials (SRM's) as defined by the National Bureau of Standards are well-characterized materials, produced in quantity and certified for one or more physical or chemical properties. They are used to assure the accuracy and compatibility of measurements throughout the nation. SRM's are widely used as primary standards in many diverse fields in science, industry, and technology, both within the United States and throughout the world. They are also used extensively in the fields of environmental and clinical analysis. In many applications, traceability of quality control and measurement processes to the national measurement system are carried out through the mechanism and use of SRM's. For many of the nation's scientists and technologists it is therefore of more than passing interest to know the details of the measurements made at NBS in arriving at the certified values of the SRM's produced. An NBS series of papers, of which this publication is a member, called the NBS Special Publication - 260 Series is reserved for this purpose.

This 260 Series is dedicated to the dissemination of information on different phases of the preparation, measurement, certification and use of NBS-SRM's. In general, much more detail will be found in these papers than is generally allowed, or desirable, in scientific journal articles. This enables the user to assess the validity and accuracy of the measurement processes employed, to judge the statistical analysis, and to learn details of techniques and methods utilized for work entailing the greatest care and accuracy. These papers also should provide sufficient additional information not found on the certificate so that new applications in diverse fields not foreseen at the time the SRM was originally issued will be sought and found.

Inquiries concerning the technical content of this paper should be directed to the author(s). Other questions concerned with the availability, delivery, price, and so forth will receive prompt attention from:

Office of Standard Reference Materials
National Bureau of Standards
Washington, D.C. 20234

George A. Uriano, Acting Chief
Office of Standard Reference Materials

TABLE OF CONTENTS

LIST OF TABLES

LIST OF FIGURES

SRM 768: Temperature Reference Standard for Use Below 0.5 K

R. J. Soulen, Jr., and R. B. Dove
Temperature Measurements and Standards Division
Center for Absolute Physical Quantities
National Bureau of Standards
Washington, D. C. 20234

Abstract

Cryogenic temperature scales are now available (viz., the newly created EPT-76 [1]) which are quite accurate and which extend deep into the cryogenic region (as low as 0.5 K). It is the region below 0.5 K where no formal scale exists which is of concern here. By developing a compact device which provides five reference temperatures from 0.015 K to 0.21 K, the authors hope to provide a *lingua franca* by which experimental results from different laboratories involving the parameter temperature may be meaningfully compared.

Such a device, designated SRM 768, is now available and consists of a self-contained assembly of coils and five samples which can be used to provide *in situ* temperature calibration. Simple room temperature electronics readily permit the observation of the five narrow and highly reproducible superconducting phase transitions. These phase transitions have been assigned temperature values by means of fundamental thermometers used at the National Bureau of Standards. Provided that care is exercised in reducing the magnetic field acting upon the device, the user can confidently expect to achieve a temperature reproducibility and traceability to the NBS temperature scale of ±0.2 mK.

Key Words: $AuAl_2$; $AuIn_2$; Be; cryogenic temperature scale; fixed points; Ir; superconductivity; thermometry; W.

I. INTRODUCTION

Cryogenic temperature scales are now available (viz., the newly-created EPT-76 [1]) which are quite accurate and which extend deep into the cryogenic region (as low as 0.5 K). It is the region below 0.5 K where no formal scale exists which is of concern here. By developing a compact device which provides five reference temperatures from 0.015 to 0.21 K, the authors hope to provide a *lingua franca* by which experimental results from different laboratories involving the parameter "temperature" may be meaningfully compared.

Such a device, designated SRM 768, is now available* and consists of a self-contained assembly of coils and five samples which can be used to provide *in situ* temperature calibration. Simple room temperature electronics readily permit the observation of the five narrow and highly reproducible superconducting phase transitions. These phase transitions have been assigned temperature values by means of primary thermometers used at the National Bureau of Standards. Provided that care is exercised in reducing the magnetic field acting upon the device, the user can confidently expect to achieve a temperature reproducibility and traceability to the NBS temperature scale of ±0.2 mK. Table I provides the salient information about SRM 768. Since the variation in T_c (typically ±1 mK) among different specimens of the same material is larger than the reproducibility of a given sample (±0.1 mK), each SRM 768 unit is accompanied by a calibration certificate.

---

*From the Office of Standard Reference Materials, National Bureau of Standards, Room B-311, Chemistry Building, Washington, D. C. 20234.

TABLE I

Summary of Properties of SRM 768

Material	Transition Temperature Will Lie Between	Typical Transition Width	Typical Reproducibility[+] Upon Thermal Cycling
	mK	mK	mK
W	15.0 - 17.0	0.7	0.20
Be	21.0 - 24.0	0.2	0.10
Ir	98.5 - 99.5	0.8	0.10
$AuAl_2$	160.0 - 161.0	0.3	0.10
$AuIn_2$	205.0 - 208.0	0.4	0.15

[+]The values given are the averages of the standard deviations of several samples.

RECOMMENDED OPERATING CONDITIONS

1) Peak-to-peak magnetic field applied in primary coil: 2.3 μT (23 mG) for W transition, 0.46 μT (4.6 mG) for the others.
2) Heating generated with above conditions: 1.8×10^{-9} W and 7.5×10^{-11} W, respectively.
3) Ambient magnetic field kept below 1 μT.

This certificate specifies each T_c in the unit to ±0.1 mK on an NBS temperature scale which is believed to be thermodynamically accurate within a few tenths of a percent from 0.01 to 0.5 K.*

In many ways SRM 768 is similar to SRM 767 [2], a device containing five superconductors whose transitions have been adopted as fixed points for EPT-76. There are significant differences between them, however, arising chiefly from the requirement of better thermal contact for SRM 768. The remainder of this publication describes in greater detail the operating conditions and instructions particular to SRM 768.

---

*This scale dubbed NBS-CTS-1 (NBS Cryogenic Temperature Scale-1) was obtained by intercomparing Co-60 gamma-ray aniosotropy and Josephson junction noise thermometers from 0.011 to 0.050 K. From 0.05 to 0.5 K the noise thermometer was used alone. The data obtained by these methods was then "smoothed" with a paramagnetic salt thermometer (cerium magnesium nitrate) to arrive at NBS-CTS-1. This scale is maintained at the NBS via secondary thermometers (germanium resistors) and two units of SRM 768 which were calibrated at the same time as the gamma-ray and noise thermometers. For a discussion of these thermometers, see H. Marshak and R. J. Soulen, Jr., Journal de Physique 39, C6-1162 (1978) and references therein.

II. SAMPLES

The physical dimensions, metallurgical state (e.g., crystallinity and state of anneal), purity and method of preparation of the five samples incorporated in the superconductive thermometric fixed-point device are quite disparate and are dictated by such considerations as toxicity and melting points of the starting materials. The relevant information on each material (W, Be, Ir, $AuA\ell_2$ and $AuIn_2$) is summarized in TABLE II. The purity of the Ir is notably low compared with the purity of the other four materials (20% Ru impurity). In fact, our experiments on different samples of all five materials have shown that specimens of higher purity can be made (at greater expense and effort!) and that in some cases the transition temperatures were different. Thus the T_c values reported for SRM 768 are not necessarily to be taken as representing the pure materials. The specific materials used for the SRM device were not chosen necessarily for their high metallurgical quality but rather for the availability of enough homogeneous material to produce many reproducible SRM units for wide distribution at a reasonable cost.

The samples were spark cut from an ingot or "boule" of each material. The surface damage caused by the cutting was removed by gentle abrasion with 600 grit silicon carbide sandpaper followed by final polishing with 20 and 2 μm diameter aluminum oxide powder. The exception to this rule was the processing of Be, which, owing to the toxicity, was used in its as-received condition. In an effort to reduce supercooling (an effect to be explained later) of the superconductive transition, small pieces of Aℓ were spot welded to one end of the Be and W samples.

TABLE II

Properties of Materials Used in SRM 768

Material	Residual Resistivity Ratio	Resistivity at 4.2 K ρ_0	Source	Sample Geometry	Purity
		Ω cm			
Tungsten	10^3	5×10^{-9}	Aremco Products, Inc. P. O. Box 429 Ossining, New York	Single crystal cylindrical rod, 0.13 cm diameter, 0.64 cm long. Cut from longer rods of same diam.	99.999%, nominal
Beryllium	79[+]	4×10^{-8}	Nuclear Materials, Inc. Cambridge, Mass	Irregular nuggets prepared by single vacuum distillation. Approximate dimensions 0.64 cm by 0.4 cm by 0.4 cm.	Detectable impurities (in ppm) are: Fe(3), Mn(5), Si(10), Al(15), N(5).
Iridium	2.5	4.4×10^{-6}	Material Research Corp. Route 303 Orangeburg, New York	Quarter-pie shapes obtained by cutting disks 0.23 cm thick from cylindrical rod of diameter 0.64 cm. The disk was then quartered. Boule was prepared by electron-beam zone refining.	Actual composition: 80% Ir; 20% Ru
$AuAl_2$	50	2×10^{-7}	Prepared at NBS[++] using 99.999% pure Al and Au	Rectangular parallelepiped l = 0.66 cm, w = 0.22 cm, t = 0.22 cm spark cut from electron beam zone refined boule.	
$AuIn_2$	50	2×10^{-7}	Prepared at NBS[++] using 99.999% pure In and Au	Rectangular parallelepiped l = 0.66 cm, w = 0.22 cm t = 0.22 cm spark cut from directionally solidified boule.	

[+]Dr. Ray Radebaugh, NBS Boulder, private communication.

[++]Prepared by Mr. Frank Biancaniello.

III. FABRICATION OF SRM 768

This device is a self-contained assembly of samples and coils permitting the observation of five superconductive transitions with a reasonable signal-to-noise ratio without generating appreciable heating, while at the same time maintaining good overall thermal equilibrium among its parts. Fig. 1 shows the arrangement which has been found to satisfy these requirements.

Two holes are drilled through a cylindrical OHFC copper block, the other end of which has been machined to form a 6-32 screw. Into each of the two holes is inserted a bundle of 300 bare AWG 40 copper wires. Each bundle is welded in place, and the surface facing the 6-32 screw is then remachined flat.* A serial number is stamped into the side of the unit near the screw. The whole assembly is electroplated with pure gold to an approximate thickness of 0.5 μm. Samples of W, Be, $AuIn_2$, $AuAl_2$ and Ir are each bound at the positions shown in the figure with GE 7031** varnish and cotton thread. Two sets of copper coils (a primary and secondary) mounted on thin phenolic tubes are slipped into the two holes in the copper block and enclose the samples. The spare gold-plated copper wire is then folded back over the coils and lashed down with thread and more GE 7031 varnish. As a consequence of this design, the coils and samples were found to be in thermal equilibrium even at the lowest transition temperature.

---

*Please note that the copper stud has been so annealed by the welding that care must be exercised to avoid damage (e.g., shearing off) during installation.

**Use of brand names throughout this article does not imply our endorsement; the particular products were used for convenience and are not necessarily optimum.

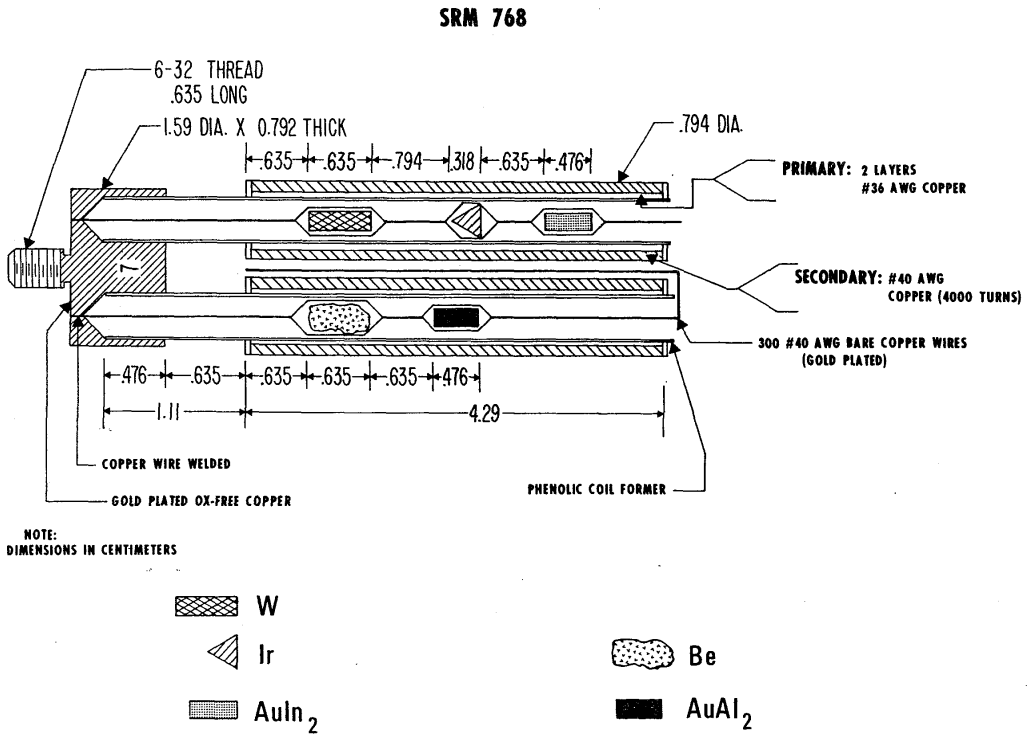

Figure 1. SRM 768. The symmetric unit is composed of two similar parts, each one consisting of two or three samples bound in copper wires inside a pair of coils (primary and secondary). The four coils are connected in series opposition so as to minimize the total mutual inductance. The serial number of the unit (in this case, 7) is stamped on the end designed for attachment to a cryostat which is terminated with a 6-32 threaded stud. The threads are relieved near the body of the device so that it will bottom properly when screwed in, thereby establishing good thermal contact.

CAUTION: Due to welding carried out in a step of manufacture, the 6-32 copper stud is well annealed and may be snapped off if too much torque is applied in mounting. "Finger tight" is sufficient.

IV. MEASUREMENT TECHNIQUES

A. Circuitry

As is shown in Fig. 1, each unit is provided with two sets of coils, each set consisting of a primary and secondary coil. The eight leads from these sets are interconnected in series opposition, however, thus requiring only four leads for measurement. The uniformity of a given pair of primary and secondary coils is such that, even though a given pair has a mutual inductance of 3 mH, the mutual inductance of the combination is generally less than 100 μH. The resistance of the combined primary coil set is about 30 Ω at room temperature and drops to 0.4 Ω at 4 K. The coil calibration of each primary coil was found to be

$$B = 0.0158\ I \qquad (1)$$

where the current I passing through the coil is given in amperes and the resulting magnetic field, B, is given in teslas. The coefficient was obtained in two ways: (1) by sending a known dc current through the coil and measuring B with a Bell gaussmeter (accurate to a few percent); and (2) by calculation using the equation for an solenoid of dimensions given in Fig. 1 knowing the turns per unit length. The two methods agreed to within 10%, and the aforementioned coil constant was taken as the average of the two values obtained.

The superconductive transitions are observed as changes in the mutual inductance of the coils which occur when the magnetic field generated by the primary coil is expelled from the interior of the sample as it enters the superconducting state (the Meissner effect). The mutual inductance change may be observed using either a Hartshorn bridge [3] or a much simplier circuit developed by one of the authors (RJS) in collaboration with J. F.Schooley and G. A. Evans [4]. The latter bridge, designed for use with SRM 767, was difficult to use with SRM 768, however. The reason for this is that the secondary coil in SRM 768 is wound directly on the primary coil in order to maintain thermal equilibrium throughout the unit. The resulting capacitance between the coils

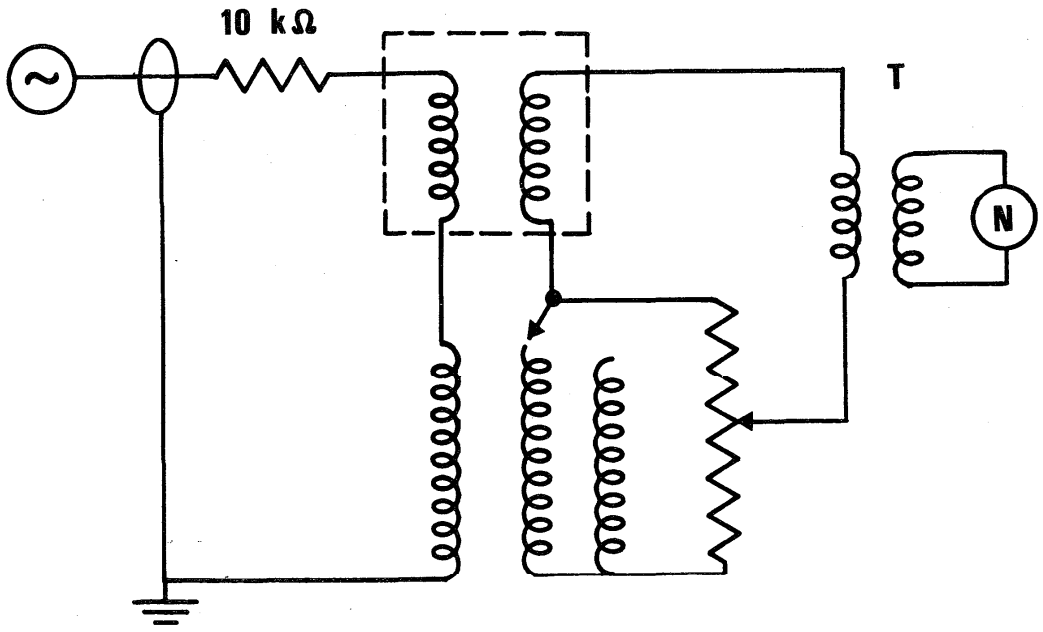

Figure 2. Mutual inductance bridge for SRM 768. The circuit shown in dashes represents the SRM 768 coils at cryogenic temperatures which are actually four coils arranged in series opposition. A switch selects one of two secondary coils of the reference mutual inductance; the one with fewer turns provides a reference mutual inductance of 0.22 mH suited for use with SRM 768, the other one gives a mutual inductance of 5.1 mH for use with SRM 767. A ten-turn potentiometer (total resistance, 100 Ω) reduces the voltage developed by the standard mutual inductance until bridge balance is achieved. A TRIAD G-4 transformer with a turns ratio of ≃ 90, couples the circuit to a phase-sensitive detector, N. We have used a PAR Model 120 phase-sensitive detector with a PAR Model 112 preamplifier as well as preamplifiers and amplifiers of our own design with equal success. Provision of a circuit to balance the small out-of-phase component of the voltage has not proved necessary.

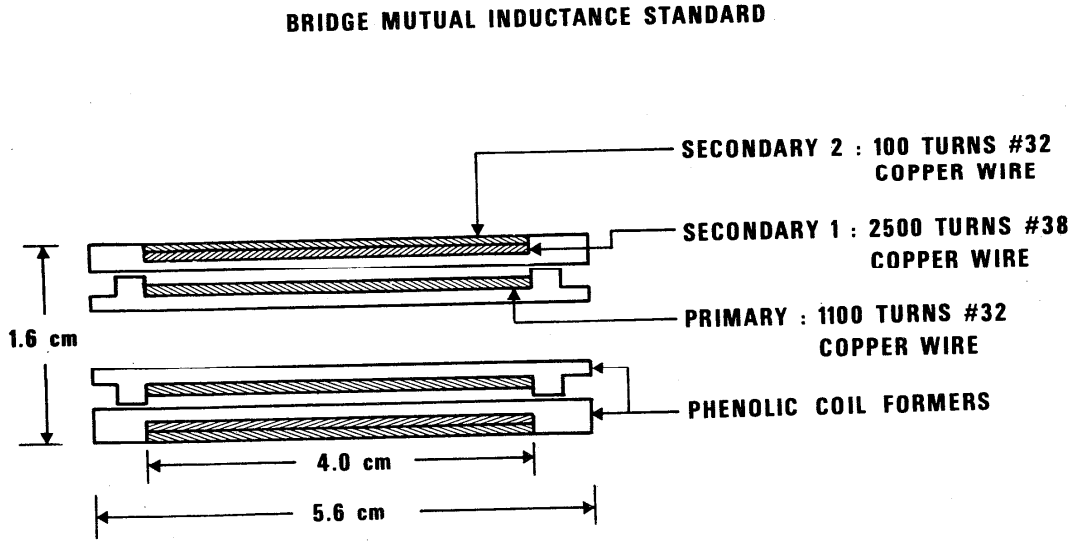

Figure 3. Standard mutual inductance. The primary coil (innermost coil) is wound on a phenolic coil former which has an inner diameter (i.d.) of 0.64 cm and an outer diameter (o.d.) of 0.80 cm. The secondary coil of 2500 turns is wound on a second phenolic former with an i.d. of 1.1 cm and an o.d. of 1.3 cm. The 100-turn secondary is wound on top of the latter coil. The mutual inductance between the primary and the 2500 turn coil is 5.1 mH, while the mutual inductance between the same primary and the 100 turn secondary is 0.22 mH.

introduces a large phase shift into the circuit which renders balancing of the bridge difficult. To circumvent this problem, the authors developed a third bridge which is relatively immune to such capacitances, performs just as well as the previous two and is as simple to build as the second. This new bridge is shown schematically in Fig. 2. It injects a current at a frequency of 400 Hz from the reference voltage of a phase-sensitive detector into the primary coil of the SRM unit as well as into the primary of a simply-constructed standard mutual inductance (see Fig. 3). The voltage induced in the secondary coil of the standard inductor is reduced by means of a ten turn potentiometer which can be adjusted to null the voltage induced in the secondary of the SRM unit. The null condition is observed with a phase-sensitive detector which is coupled to the circuit by a transformer, T. The circuit parameters used here are not necessarily optimized, but the authors have found that this bridge performs as well as the two aforementioned bridges.

A typical superconductive transition is shown in Fig. 4. The output from the phase-sensitive detector, which is proportional to the change in mutual inductance of the coil set (in arbitrary units), is plotted on the Y axis of an X-Y recorder, while on the X axis is registered the offset of an ac resistance bridge which monitors a calibrated germanium resistance thermometer. The width, W, of the transition is defined as the temperature range over which 80% of the change in mutual inductance occurs, while the T_c is defined as the midpoint of the mutual inductance change. For this sample of iridium, $W \simeq 0.9$ mK, and $T_c \simeq 0.098$ K. Two traces of the transition are generally obtained, one as the sample is slowly warmed through the transition, and a second as the sample is cooled back through T_c. The hysteresis could be due either to lack of thermal equilibrium between the sample and the resistance thermometer or to supercooling effects. Experiments quickly showed that, as long as heating (cooling) rates were slower than 0.5 mK/min, the hysteresis which appeared in all the materials was due to supercooling and not to lack of thermal equilibrium. All data reported here were obtained with heating (cooling) rates less than this value.

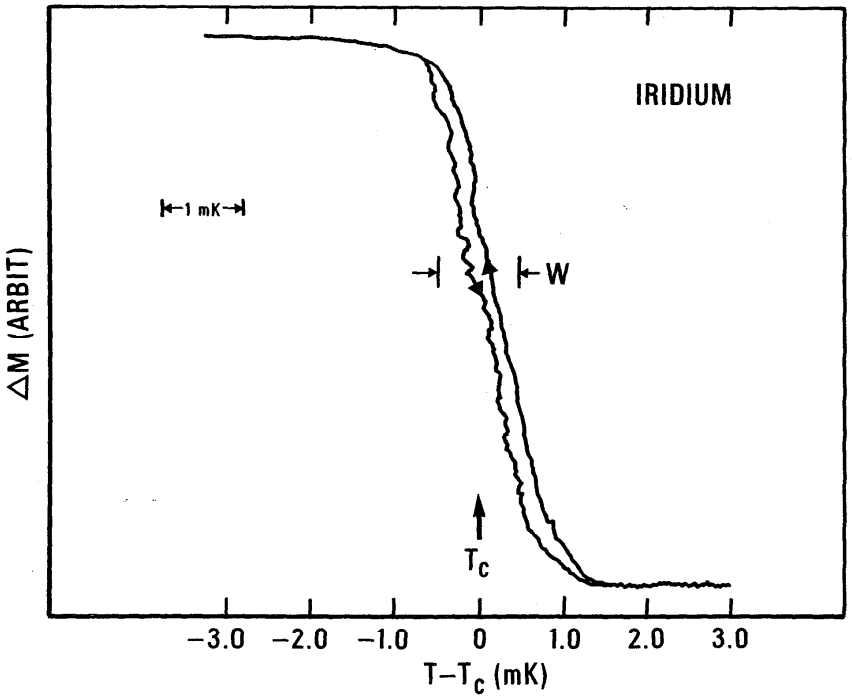

Figure 4. Iridium phase transition. The change in mutual inductance ΔM as observed by the circuit in figure 2 is plotted in arbitrary units versus the output of an ac resistance bridge monitoring a calibrated germanium resistance thermometer. The transition temperature is chosen as the midpoint of the transition, while the width W of the transition is defined as 80% of the change ΔM centered about T_c. This transition was plotted out in a time of approximately five minutes. The slight amount of hysteresis present is due to supercooling.

It is worth pointing out that a simplification in the measurement process ensues from this particular arrangement of samples and coils. Note in Fig. 1 that the samples are placed in the coils so that, as the temperature is raised or lowered, the occurrence of a superconductive transition will alternate back and forth between the two coil sets. Since the change in mutual inductance produced by four of the samples (W is the exception) is about the same magnitude, and since the coils are arranged in series opposition, the output on the Y axis of the X-Y recorder will be displaced first in one direction by the first transition, then returned approximately to the original position by the second, and so on. This means that rebalancing of the bridge after each transition and changing of the amplifier gain are not really necessary in order to measure the transitions of Be, Ir, $AuAl_2$ and $AuIn_2$. The mutual inductance change accompanying the transition in the tungsten sample is about a factor of 25 less than the others, however, and the gain must be increased accordingly.

B. Heating: the effect of ac magnetic fields

Since SRM 768 is intended for use at very low temperatures where even very small amounts of heat are perceptible, a natural question concerning the use of the device is, "How much current can be used in the primary coil to observe the transition and, How much heat is generated?" Actually, introduction of current into the primary coil generates heat in three ways: the familiar I^2R loss in the primary coil, eddy current heating in the samples, and eddy current heating in the gold-plated copper wires used to enclose the samples. Calculation of the first is obvious: the eddy current heating can be calculated from the equation [5]

$$\dot{Q} = \frac{V}{32\rho} \overline{\dot{B}^2} \, d^2 \, 10^{-16} \, W \qquad (2)$$

where V is the sample volume exposed to a time-varying magnetic field, $\dot{B}$. The resistivity of the sample is given by ρ and d is the diameter of the sample. Assuming $B = B_o e^{i\omega t}$, and averaging over one cycle, we obtain

$$\overline{\dot{B}^2} = \frac{B_o^2}{2} 4\pi^2\nu^2 = \frac{B_{pp}^2}{8} 4\pi^2\nu^2 \qquad (3)$$

Here we have used the peak-to-peak value, B_{pp}, instead of B_o, since peak-to-peak voltages are easy to determine from oscilloscope traces. Equation (2) thus becomes

$$\dot{Q} = \frac{V B_{pp}^2 \pi^2}{64\rho} \nu^2 d^2 10^{-16} W \qquad (4)$$

The eddy-current heating was calculated for two values of magnetic field because these are the ones recommended for observation of the superconductive transitions in SRM 768. That is to say, a value of B_{pp} = 0.46 μT has been found to produce a voltage change of between 20 and 50 μV at the output of the coupling transformer (see Fig. 2) when the Be, Ir, $AuAl_2$ and $AuIn_2$ transitions occurred. This signal produces a trace on the Y axis of the recorder with a signal-to-noise (S/N) ratio of at least 10/1 when a time constant of 1 s is used. Since the signal induced by the W transition is about a factor of 25 weaker, both the amplitude of the magnetic field and amplifier gain can be increased by factors of five. In this case, the vertical axis signal of the X-Y recorder was observed to have a S/N ratio of at least 5/1 and thus the W transitions were readily observable. Equation 4 was used to estimate the three heating terms of these two values of magnetic field, and the results are summarized in TABLE III.

TABLE III

Heating in SRM 768

Material	V^{+}	d^{++}	ρ_o	$\dot{Q}$ ν = 400 Hz I_{pp} = 29 μA B_{pp} = 0.46 μT[+++]	$\dot{Q}$ ν = 400 Hz I_{pp} = 140 μA B_{pp} = 2.3 μT[+++]
	cm^3	cm	Ω cm	W	W
W	8.0×10^{-3}	0.13	5×10^{-9}	1.4×10^{-12}	3.6×10^{-11}
Be	7.3×10^{-2}	0.40	4×10^{-8}	3.1×10^{-11}	7.9×10^{-10}
Ir	1.8×10^{-2}	0.20	4.4×10^{-6}	8.6×10^{-15}	2.2×10^{-13}
$AuAl_2$	3.5×10^{-2}	0.20	2×10^{-7}	3.8×10^{-13}	9.3×10^{-12}
$AuIn_2$	3.5×10^{-2}	0.20	2×10^{-7}	3.8×10^{-13}	9.3×10^{-12}
			SUBTOTAL	3.3×10^{-11}	8.4×10^{-10}
600 #40 AWG copper wires	1.3×10^{-1}	7.5×10^{-3}	3×10^{-8}	1.0×10^{-13}	2.6×10^{-12}
			SUBTOTAL	3.3×10^{-11}	8.4×10^{-10}
I^2R Heating[++++]				4.2×10^{-11}	9.8×10^{-10}
			TOTAL	7.5×10^{-11}	1.8×10^{-9}

\+ Sample volume, V, calculated from dimensions given in TABLE II.

++ If the sample did not have a circular cross section, a fictional diameter d was obtained by setting $A = \pi d^2/4$, where A is the cross-sectional area of the sample.

+++ Obtained from the coil constant, B = 0.0158 I.

++++ The resistance, R, of the two primary coils at 4.2 K is 0.4 Ω; the average power per cycle is $\bar{I}^2R = I_{pp}^2 R/8$.

Several approximations render entries in TABLE III somewhat uncertain. We have approximated non-cyclindrical rod samples by a simulated cylindrical geometry of the same cross section. Variation of resistivity and volume of the samples could cause the estimate of eddy current heating in the samples to vary by as much as 20%. Moreover, the calculation of the eddy-current heating generated in the 300 copper wires assumes that all wires are electrically insulated from each other. In actual fact they do touch each other by virtue of the construction and the resulting increase in heating is hard to estimate. In view of these uncertainties, an experiment was conducted with five SRM 768 units connected in series on a common copper platform which also held a calibrated germanium resistance thermometer to determine whether such heating, though small, could be observed. With this arrangement the estimates for heating given in TABLE III should be multiplied by an additional factor of five. The transitions of the five samples each of W, Be, Ir, $AuAl_2$ and $AuIn_2$ were first recorded on the germanium resistance thermometer (i.e., 25 X-Y recordings) using a peak-to-peak primary field of 0.46 μT; then all 25 transitions were recorded (with a reduction in amplifier gain) using a field of 2.3 μT. If the aggregate effect of the terms given in TABLE III were important, the T_c values should systematically shift when the peak-to-peak field was quintupled. No shift in temperature greater than the imprecision of the measurement (about 0.05 mK) was observed in any of the twenty-five samples. We conclude that the heat generated in the measurement of the T_c's does not produce any noticeable temperature gradient between the specimens and thermometer as long as thermal contact is established via a metallic link. If, however, a liquid-solid interface (e.g., liquid He^3-copper) separates the SRM unit from the desired thermometer, as can commonly occur in dilution refrigerator applications, greater care may have to be exercised.

C. The effect of dc magnetic fields on SRM 768

The single most important environmental factor which determines the shape and position of the superconductive transition is the ambient magnetic field. We discern two distinct effects here.

In the first place, the magnetic field $H_c(T)$ which completely suppresses superconductivity at a temperature T in a sample is given approximately by [6]

$$H_c(T) \simeq H_c(0)\ (1-(T/T_c)^2) \tag{5}$$

The more accurate equation, differing by a few percent from Eqn. 5, is given by the BCS theory [7]. Thus, if an ambient magnetic field of value H_a is present, Eqn. 5 or the more correct BCS function can be solved for the temperature T_c' (by necessity, below T_c) at which the superconductive transition will now occur. The effect on the transition curve shown in Fig. 4 is to uniformly displace the curve to a lower temperature. Near T_c this displacement may be calculated from

$$\Delta T_c = T_c' - T_c = H_a \left(\frac{dH_c}{dT}\right)^{-1}_{T=T_c} \tag{6}$$

The slope of the critical magnetic field can be calculated from the BCS result [7]

$$\left(\frac{dH_c}{dT}\right)_{T=T_c} = 1.737 \left(\frac{H_c(0)}{T_c}\right)(1-\bar{a}^2) \tag{7}$$

Here $\bar{a}^2$ is the average of the energy gap anisotropy parameter which, at risk of committing errors of 1-2%, we set to zero.

The second effect of the same magnetic field is to cause the sample to supercool: that is, the sample must be cooled considerably below the equilibrium T_c' before it can enter the superconducting state. This effect introduces hysteresis into the transition as it is traced out. The maximum supercooling that can occur can be calculated from the equation derived from the Ginzburg-Landau theory [8]

$$H_{sc} = H_a = 2.4\ \kappa H_c(T) \tag{8}$$

where the G-L parameter κ is given in terms of other solid state parameters of the superconductor [9]

$$\kappa = \kappa_o + \kappa_i \tag{9}$$

where

$$\kappa_o = 1.61 \times 10^{24} \left(\gamma^{3/2} T_c / N^{4/3}\right) \left(\frac{S_f}{S}\right) \tag{10}$$

and

$$\kappa_i = 7.53 \times 10^3 \rho \gamma^{\frac{1}{2}} \tag{11}$$

Here, γ is the linear coefficient of the normal-state electronic specific heat, N is the number of valence electrons per unit volume, S is the free area of the Fermi surface, and S_f is the area of the Fermi surface for a free-electron gas of density N. Thus κ may be evaluated for each material using normal state values, and the maximum amount of supercooling (i.e., how low the temperature must be reduced for superconductivity to occur) may be calculated from Eq. (8) and solving for the supercooling temperature T_s.

Near T_c, the amount of supercooling can be evaluated by

$$\Delta T_s = T_s - T_c = \frac{1}{2.4\kappa}\left(\frac{dH_c}{dT}\right)^{-1}_{T=T_c} H_a \tag{12}$$

We note an important point: this expression gives the *maximum* supercooling which can occur. Sample imperfections will cause the sample to enter the superconducting state anywhere between T_s and T_c.

Both effects, depression of the transition and supercooling, were studied for each material used in SRM 768. A typical measurement is shown in Fig. 5 for Be. The curve with the highest superconducting transition and minimum hysteresis was recorded by cancelling all three components of the earth's magnetic field with a three-axis Helmholtz coil. Curves with depressed transitions and supercooling were generated by applying known values of magnetic field along the axis of the measuring coil set. From such curves, it was possible to obtain experimental values of $(dH_c/dT)_{T=T_c}$ and κ. These are given in TABLE IV along with the theoretical estimates using the appropriate equations and parameters. Except for the case of $AuAl_2$, the experimental and theoretical values for the slope are in good agreement. Thus Eqn. (6) can be used to calculate the depression in transition with great confidence. We

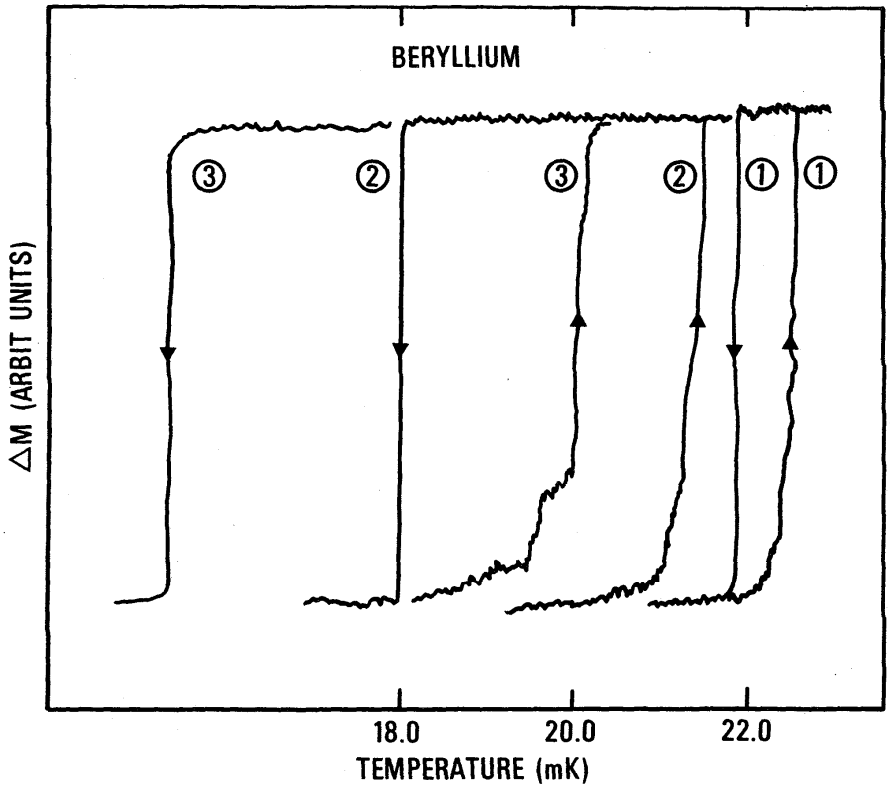

Figure 5. The effect of magnetic field on the transition in Be.

		T_c	T_s
Curve 1:	H = 0.0 T	22.7 mK	22.0 mK
Curve 2:	H = 9.5 μT	21.3	18.0
Curve 3:	H = 19 μT	20.0	15.4

TABLE IV

Magnetic Values of SRM

Material	T_c[a]	$H_c(0)$	$\left(\frac{dHc}{dT}\right)^{theor.}_{T=T_c}$[f]	$\left(\frac{dHc}{dT}\right)^{expt.}_{T=T_c}$	$\kappa^{theor.}$[g]	$\kappa^{expt.}$	ΔT_c for 1 μT	ΔT_s for 1 μT no Al spot welds	ΔT_s for 1 μT Al spot welds
	mK	10^{-4}T	μT/mK	μT/mK			mK	mK	mK
W	16.0	1.20[b]	13.0	11.6	4×10^{-3}	0.09	0.08	0.36	0.04
Be	23.1	1.14[c]	8.6	7.0	10^{-2}	0.13	0.14	0.46	0.05
Ir	99.0	-[d]	-	13.0	2.1	2.1	0.08	0.02	0.02
$AuAl_2$	160.5	12.1[e]	13.1	7.9	5×10^{-2}	1.6	0.13	0.03	0.03
$AuIn_2$	207.0	14.5[e]	12.2	12.5	4×10^{-2}	0.07	0.08	0.48	0.48

a. Average values obtained from data in this work.

b. The average of the value 1.15×10^{-4} T obtained from W. C. Black, R. T. Johnson, and J. C. Wheatley, J. Low Temp. Phys. 1. 1, 641 (1969) and 1.24×10^{-4} T obtained from B. B. Triplett, N. E. Phillips, T. L. Thorp, D. A. Shirley, and W. D. Brewer, J. Low Temp. Phys. 12, 499 (1973).

c. Calculated from another BCS relation

$$2 \pi \gamma (T_c/H_c(0))^2 = 1.057$$ where the value for $\gamma = 414.5$ ergs/cm^3 K was used based on averaging the results of R. W. Hill and P. L. Smith, Phil. Mag. 44, 636 (1953) and E. Gmelin, Comptes Rend. 259, 3459 (1964).

d. Sample is a type II superconductor; see D. U. Gubser and R. J. Soulen, Jr., J. Low Temp. Phys. 13, 211 (1973).

e. R. J. Soulen, D. B. Utton, and J. H. Colwell, Bull. Amer. Phys. Soc. 22, 403 (1977).

f. Evaluated using Eqn. 7 and the parameters given in the first two columns of this table.

g. Calculations used equations 10 and 11 and a number of sources for the solid state parameters.

note that the theoretical value for κ is always less than its experimental value, which says that none of the samples supercools to its theoretical maximum. Clearly, in calculating the effect of supercooling for the samples in SRM 768, Eqn. (12) is to be used with the *experimental* values for κ.

The last two columns in TABLE IV give values for depression of T_c and supercooling which will actually be seen in an ambient magnetic field of 1 μT. For example, in that magnetic field, the superconductive transition of tungsten will be depressed by only 0.08 mK, but the sample will have to be cooled yet another 0.36 mK before it becomes superconducting. Since the supercooling is very much larger than the depression of T_c for a given value of magnetic field, it is possible for larger fields to supercool the sample to absolute zero, thereby making observation of the transition impossible even though T_c is finite! The supercooling is especially large for W and Be so the authors adopted the procedure of spot welding two small buttons of pure aluminum (99.999 percent pure) to one end of each sample of these two materials.*

---

*This was accomplished by charging a 4500 μFd capacitor to 30 V and discharging it through the pure Aℓ wire (diameter $\simeq$ 2.4×10^{-2} cm) and a W or Be sample. This technique deposited an Aℓ hemisphere approximately 2.5×10^{-2} cm in diameter onto the sample. We found that we could restrict the superconductor in a more clearly-defined geometry by this technique than by soldering.

Aluminum, possessing a higher T_c ($\simeq$ 1 K) and H_c ($\simeq$ 10,000 μT) serves as a nucleation center to induce superconductivity in the samples. We observed that the supercooling in samples so treated was reduced by an order of magnitude. The last column in TABLE IV indicates the supercooling which can actually be expected for SRM 768. To summarize: a 1 μT field does not produce much supercooling, but it still leads to significant reductions in T_c. We would therefore recommend for the highest thermometric accuracy that ambient magnetic fields be reduced to at least this value by techniques to be described in the next section.

V. PERFORMANCE OF SRM 768

A. Cryogenic testing apparatus

In this section we describe our experience with eight SRM 768 units which were cycled several times between room temperature and 0.01 K. These experiments, with a few exceptions, extended only over a period of several months and therefore provide little information on long-term performance. These experiments, however, are the culmination of a four year program in which several other samples of these materials (not necessarily from the same source or boule) have been used for several years during which no evidence was found to indicate that reproducibility of a given sample would degrade with age or thermal cycling.

The cryostat used for these experiments is a He^3- He^4 dilution refrigerator which can maintain temperatures as low as 0.01 K in its continuous mode of operation. The general features of the cryostat are: an outer glass dewar containing liquid N_2 and an inner glass dewar containing liquid He^4 at a temperature of 4 K. A brass vacuum can, 60 cm long and 8.9 cm in diameter, is immersed in the liquid He^4 and contains a pumped He^4 bath at 1 K and a dilution refrigerator. The remaining volume inside the can (about 30 cm long and 8.9 cm in diameter) provides the working space for the experimental samples.

The cryostat was cooled in the following way. At room temperature the vacuum can was pumped to a pressure of approximately 0.13 Pa (1μm of Hg) and then filled with He^3 exchange gas at a pressure of 67 Pa.

The liquid nitrogen dewar was filled and maintained full overnight, thereby cooling the apparatus to 77 K. Subsequent transfer of liquid He^4 into the inner dewar reduced the temperature to 4 K. The vacuum can was then pumped for 30 minutes, after which heaters warmed the 1 K pot and dilution refrigerator to 10-15 K. This "bakeout" proceeded for another 30 minutes to reduce the He^3 pressure to 1.3×10^{-4} Pa as read on a room temperature ionization gauge. After this the heaters were turned off and the charge of ^3He - ^4He gas was condensed into the dilution refrigerator. Then circulation of the refrigerator was begun and the mixing chamber was eventually cooled to $\simeq$ 10 mK.

The ambient magnetic field at the site of the cryostat is approximately 5×10^{-5} T; two means have been used to reduce it to a level tolerable to the SRM 768 unit. When studies of the magnetic field dependence were desired, the dewars were surrounded with three Helmholtz coils arranged on three orthogonal axes. When minimization of the magnetic field was desired, two annealed concentric mu metal cylindrical shields were used. The inner one is 60 cm long, fits on the brass vacuum can, and is thus maintained at 4 K. The outer one is also 60 cm long and slips on the outside of the N_2 dewar (diameter 20 cm). Assuming a magnetic permeability of 10,000 we calculate that the ambient field should be attenuated by a factor of 2400 by the two mu metal cans when they are both at room temperature. Thus the magnetic field at the site should be reduced to 2×10^{-8} T using these cans. A value of 1×10^{-8} T was actually achieved when the cans were removed from the cryostat and separate coils around each cylinder were used to "degauss" the cans *in situ*. Unfortunately, when the cans are mounted on this particular cryostat, there is no room for a coil to surround the inner can, so the cans must be degaussed in the following sequence: removal of the outer can from the N_2 dewar; degaussing the inner can; then raising the outer mu metal can and degaussing both in place. In this situation the magnetic field inside the cans is found to vary from 0.1 to 0.2 μT at room temperature. A further degradation in the shielding is expected to occur when the inner mu metal can is cooled to 4.2 K, because the permeability drops by a factor of ten. We therefore estimate that the

samples are exposed to a residual field of 1 to 2 μT under the conditions of a degaussing at 300 K followed by cooling of the inner can to 4 K. This situation could be improved by constructing the inner cylinder from a material whose permeability is not reduced at 4 K, but inspection of TABLE IV indicates that a magnetic field of 2 μT is tolerable, though not desirable.

Some authors have suggested using superconducting shields to reduce the magnitude of the ambient magnetic field, but we strongly recommend that this technique not be used. The problem is that thermal gradients in the shield generate large currents and magnetic fields as the shield enters the superconducting state. Thus the experimentalist can find himself confronted with a cryogenic environment "poisoned" by a field of several mT even though he began the experiment at liquid nitrogen temperatures with a field of a few μT! [10]. Given the relative ease in elimination of fields by the other two techniques described above, we feel that the use of superconductive shields in this context introduces an unnecessary risk.

In Fig. 6 we show a schematic diagram of the bottom of the mixing chamber. The dilution refrigerator (i.e., still, heat exchangers, mixing chamber) is a commercial version in which the bottom of the mixing chamber has been replaced by one of our own design and fabrication. The bottom used here is a solid piece of OFHC copper which has been plated to a thickness of 0.5 μm with pure gold after all holes were drilled and tapped. Several 6-32 holes are tapped in the upper section, four of which accept doped germanium resistance thermometers (GERT's for short) which were inserted into gold-plated copper pods made to our specifications. Two of these resistance thermometers (Serial #2966 and 15151) were usable down to 0.1 K, below which the resistance of the thermometers grew too large for use (several MΩ), while two others (Serial #RS2 and 1405) were sensitive down to 0.01 K and relatively insensitive above 0.1 K. The lower section of this assembly consists of a rod which terminates in a blind hole which can accept a gold-plated mating post. A nylon compression clamp completes the junction. Since the bottom of the dilution refrigerator is fabricated from a single

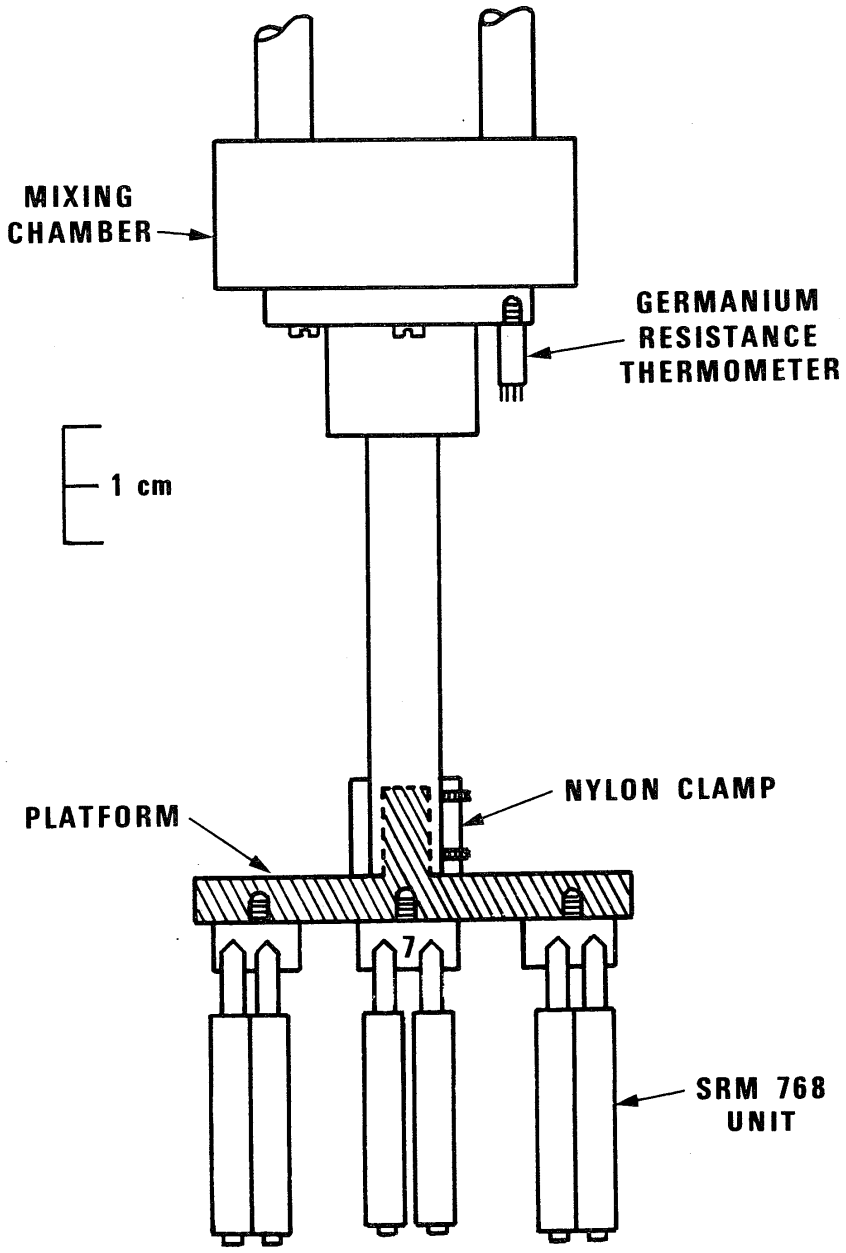

Figure 6. Bottom of dilution refrigerator with thermal platform.

piece of annealed copper, it can be considered isothermal in all thermometry experiments conducted in this apparatus. Furthermore, no perceptible thermal gradients across the connector at the bottom of the rod have been observed.

The desired experimental apparatus is mounted to the post. For example, when it was desirable to calibrate the GERT's, a Josephson junction noise thermometer was clamped around the post and a γ-ray anisotropy thermometer was slipped into the blind hole and clamped. On other occasions, a paramagnetic salt, cerium magnesium nitrate (CMN), was mounted to a post which fitted into the blind hole. Over the course of years and several experiments of this nature, an absolute temperature scale of high accuracy has been achieved and transferred to the GERT's. This temperature scale, designated NBS-CTS-1 and to be fully described elsewhere, was used to assign values to the superconductive transitions in SRM 768. Its maximum thermodynamic inaccuracy is believed to be a few tenths of a percent over its range of 0.01 K to 0.5 K.

When superconductive transitions were to be measured, the primary thermometers (noise, γ-ray) were removed and a copper platform containing SRM 768 units was attached to the connector. The GERT's, retaining the temperature scale, were used to define the temperatures of the transitions. The platform shown in Fig. 6 consists of a solid copper structure in the form of a copper disk (diameter 7.5 cm; thickness 0.6 cm) terminating in a post which fits into the connector. Several 6-32 holes are tapped in the disk and a gold plate of 0.5 μm thickness covers all surfaces of the platform.

In the experiments reported here, as many as five SRM 768 devices were screwed into 6-32 tapped holes in the platform and, for economy of electrical leads, the primary coils were connected in series. To expedite the measurements five measurement bridges, phase sensitive detectors, and X-Y recorders were used so that the transitions of a given material in all five devices could be simultaneously traced out on a common temperature scale determined by the most senior GERT (Serial #1405). The width and hysteresis of each transition were thereby obtained in terms of GERT #1405. After complete tracings were obtained, the center of one of the transitions was measured versus as many of the four GERT's as were usable at that temperature. The centers of the other transitions were then determined relative to the center of that unit from the X-Y recordings.

The GERT's were measured with an ac Mueller bridge operated at 27 K. Below 0.1 K, a peak-to-peak voltage drop of 80 μV was maintained across the resistors, while above 0.1 K the voltage drop was increased to 160 μV. At these levels of excitation, no self-heating of the GERT's to the μK level was observed, yet adequate temperature sensitivity of approximately 50 μK was maintained. The output of the preamplifier connected to the bridge was monitored to establish that extraneous noise (chiefly 60 Hz) was kept below 1 μV (peak-to-peak) even though the resistances of GERT #1405 and RS2 increase to values as high as 400 kΩ at 10 mK. Thus extraneous power generated in the resistors was $(1/80)^2$ less than that purposely generated by the signal at 27 Hz. Such low noise was only achieved by careful circuit design, generous use of mu metal shields around electronic components, and careful location of electronic equipment.

B. Analysis of data

Two groups of prototype SRM 768 units were prepared. The first group with Serial Nos. 1, 2, 3 contained W and Be samples with no Aℓ spot welds to suppress the supercooling. The second group (Serial Nos. 7, 8, 9, 10, 11) used the Aℓ spot welds for these two materials and a different boule of $AuIn_2$. The results for the first group (1, 2, 3) are shown in Table V, while the results for the second (7, 8, 9, 10, 11) are given in Table VI. A typical entry reads as follows: for the tungsten sample in SRM 768, Serial No. 1, in run I, the transition temperature was measured to be 15.37 mK, the width of the transition was 0.21 mK and it had a hysteresis due to supercooling of $\simeq$ 0.04 mK.

There are some blanks in Table V for the W samples which indicate that the supercooling was so large on these occasions that the sample remained in the normal state to the lowest temperature obtainable with the dilution refrigerator ($\simeq$ 10 mK). No such entries occur for the W samples in Table VI, indicating that the hysteresis due to supercooling was successfully reduced by the Aℓ spot welds. Also note that the hysteresis (reported in the last column) was significantly reduced for Be by the application of Aℓ spot welds. It is evident that supercooling is not a problem for the other materials in SRM 768. In Table VI there are no entries for $AuIn_2$ samples for runs 1-4 because a new sample preparation technique was tried here which produced poor samples. In runs 5-11, samples of $AuIn_2$ were prepared in the original way used for units 1, 2, 3, except that a new boule of $AuIn_2$ was used.

We note also that the T_c values of $AuIn_2$ for the first group (1, 2, 3) are about 2 mK higher than for the second group (7, 8, 9, 10, 11) indicating that there is some variation in T_c from boule to boule. It is also apparent, however, that each boule yields quite uniform T_c values.

TABLE V

Reproducibility of Early SRM 768 Units (Serial No. 1, 2, 3)

SAMPLE	T_c Run 1 (9/15/76)	T_c Run 2 (9/28/76)	T_c Run 3 (11/24/76)	T_c Run 4 (12/8-16/76)	T_c Run 5 (8/4/78)	Average T_c	Standard Deviation	Width W	Hysteresis
	mK	mK	mK	mK	mK	mK	mK	mK	mK
W-1	15.37	15.45	15.61	15.62	-	15.51	0.12	0.205	0.041 - 0.11
W-2	15.33	15.14	15.49	15.64	-	15.41	0.21	0.27	0.07
W-3	+	+	15.80	16.26	16.70	16.25	0.45	0.27	0.7
Be-1	21.28	+++	22.15	23.01	-	22.15	0.86	0.06	0.7 - 1.4
Be-2++	23.10	+++	23.01	22.48	-	22.86	0.33	0.06	0.2 - 1.2
Be-3++	24.02	+++	24.8	+++	+++	24.41	0.55	0.05	2.5 - 4.5
Ir-1	98.66	98.61	98.72	98.80	-	98.69	0.08	0.4	<0.1
Ir-2	98.84	98.82	99.00	99.05	-	98.92	0.11	0.4	<0.1
Ir-3	98.54	98.39	98.46	98.64	98.78	98.56	0.15	0.7	<0.1
$AuAl_2$-1	160.63	160.38	160.60	160.83	-	160.60	0.18	0.4	<0.1
$AuAl_2$-2	160.38	160.21	160.46	160.71	-	160.45	0.21	0.8	<0.1
$AuAl_2$-3	160.71	160.38	160.71	160.88	161.05	160.74	0.25	0.09	<0.1
$AuIn_2$-1	207.36	207.28	207.52	207.69	-	207.44	0.18	0.3	<0.1
$AuIn_2$-2	207.16	207.08	207.24	207.48	-	207.24	0.17	0.2	<0.1
$AuIn_2$-3	207.48	207.08	207.36	207.65	207.69	207.44	0.25	0.2	<0.1

+ The hysteresis due to supercooling was too large to permit a measurement of T_c.

++ Be-3 was taken from a different source of beryllium.

+++ The T_c values were not measured during that run, even though the transition was observable.

- Not included in the experiment.

TABLE VI

Reproducibility of later SRM 768 Units (Serial No. 7, 8, 9, 10, 11)

SAMPLE	T_c Run 1 4/21/78	T_c Run 2 4/24/78	T_c Run 3 4/28/78	T_c Run 4 5/3/78	T_c Run 5 6/14/78	T_c Run 6 6/20/78	T_c Run 7 6/27/78	T_c Run 8 6/30/78	T_c Run 9 7/6/78	T_c Run 10 7/11/78	T_c Run 11 7/12/78	Runs 1-4 s	Runs 1-4 $\overline{(T_c)}$	Runs 5-11 s	Runs 5-11 $\overline{(T_c)}$	$s/\sqrt{N}$	Width W	Hysteresis
	(mK)	(mK)	(mK)	(mK)	(mK)	(mK)	(mK)	(mK)	(mK)	(mK)	(mK)	(mK)	(mK)	(mK)	(mK)	(mK)	(mK)	(mK)
W-7	16.39	-	16.39	-	16.09	16.09	16.17	16.26	16.22	15.99	15.76	0.00	16.39	0.17	16.08	0.06	0.29	0.07
W-8	16.44	-	16.28	-	16.05	15.85	16.30	16.24	16.17	15.99	15.66	0.11	16.36	0.23	16.03	0.09	0.18	0.07
W-9	16.92	-	16.55	-	16.27	16.21	16.51	16.59	16.48	16.21	16.08	0.29	16.62	0.19	16.34	0.07	1.36	0.14
W-10	16.91	-	16.56	-	16.23	15.75	15.80	15.82	16.01	15.39	15.98	0.25	16.74	0.26	15.85	0.10	1.50	0.04
W-11	17.11	-	16.73	-	16.42	-	16.75	16.67	16.57	16.44	16.21	0.27	16.92	0.19	16.51	0.07	1.50	0.04
Be-7	23.31	23.35	23.19	-	23.06	23.06	23.04	23.01	23.02	23.01	22.97	0.06	23.25	0.03	23.02	0.01	0.13	<0.08
Be-8	23.25	23.29	23.04	-	23.12	23.04	23.09	22.97	23.04	23.04	23.01	0.13	23.19	0.05	23.04	0.02	0.25	<0.06
Be-9	23.12	23.27	22.95	-	22.61	22.41	22.43	22.20	22.39	22.38	22.72	0.16	23.1	0.17	22.44	0.06	0.27	0.27
Be-10	23.67	23.37	23.21	-	23.02	23.06	23.04	23.08	23.16	23.10	23.25	0.23	23.42	0.08	23.10	0.03	0.23	0.22
Be-11	23.33	23.67	23.35	-	23.27	23.23	23.18	22.99	23.04	22.97	23.01	0.19	23.45	0.12	23.10	0.05	0.30	0.18
Ir-7	99.33	99.33	99.36	-	99.41	99.37	99.37	99.21	99.37	99.47	99.40	0.017	99.34	0.08	99.37	0.03	0.83	<0.1
Ir-8	99.23	99.20	99.09	-	99.23	99.09	99.20	99.07	99.17	99.34	99.21	0.074	99.17	0.10	99.19	0.04	0.87	<0.08
Ir-9	99.00	98.96	98.97	-	99.05	98.95	98.98	99.20	99.13	99.11	99.07	0.021	98.98	0.09	99.07	0.03	0.90	0.13
Ir-10	99.07	98.97	98.97	-	99.16	99.03	98.98	98.84	99.15	99.10	99.01	0.058	99.00	0.11	99.03	0.04	1.20	0.21
Ir-11	98.93	98.84	98.90	-	99.01	98.91	98.91	98.72	99.13	99.02	98.88	0.046	98.89	0.13	98.94	0.05	1.10	0.22
$AuAl_2$-7	160.46	160.51	160.48	-	160.53	160.48	160.46	160.26	160.48	160.63	-	0.025	160.48	0.12	160.47	0.05	0.22	<0.05
$AuAl_2$-8	160.49	160.61	160.54	-	160.71	160.56	160.58	160.28	160.61	160.76	-	0.060	160.55	0.17	160.58	0.07	0.35	<0.05
$AuAl_2$-9	160.46	160.61	160.46	-	160.51	160.28	160.43	160.49	160.46	160.61	-	0.086	160.51	0.11	160.46	0.04	0.37	<0.03
$AuAl_2$-10	160.53	160.48	160.49	-	160.49	160.48	160.43	160.33	160.45	160.63	-	0.026	160.50	0.10	160.46	0.04	0.23	<0.03
$AuAl_2$-11	160.40	160.58	160.49	-	160.54	160.49	160.46	160.28	160.53	160.68	-	0.09	160.49	0.13	160.49	0.05	0.28	<0.03
$AuIn_2$-7	-	-	-	-	205.45	205.37	205.30	205.14	205.37	205.53	-			0.13	205.36	0.05	0.42	<0.04
$AuIn_2$-8	-	-	-	-	205.81	205.61	205.61	205.37	205.69	205.85	-			0.17	205.65	0.07	0.40	<0.06
$AuIn_2$-9	-	-	-	-	205.61	205.06	205.14	204.91	205.22	205.41	-			0.25	205.22	0.10	0.38	<0.04
$AuIn_2$-10	-	-	-	-	205.73	205.65	205.57	205.33	205.61	205.81	-			0.16	205.61	0.07	0.34	<0.04
$AuIn_2$-11	-	-	-	-	205.34	204.91	205.26	204.98	205.30	205.45	-			0.21	205.21	0.09	0.30	<0.04

Two techniques for degaussing the mu metal cans were tried. For runs 1-4 on units 1, 2, 3 and for runs 1-4 of units 7, 8, 9, 10, 11, degaussing was not performed until the inner shield was at 4 K. For run 5 of units 1, 2, 3 and runs 5-11 of units 7, 8, 9, 10, 11, the degaussing procedure was done at 300 K with no further degaussing at lower temperatures. We can see that for samples with Aℓ spot welds (7, 8, 9, 10, 11) there is no significant difference in T_c or in the standard deviation of T_c. When the hysteresis of the curves is examined in some detail for all units (these data are not included in this report), we find that there is generally less hysteresis in the transitions when the second technique for degaussing the mu metal cans is used. We have therefore decided to adopt the second practice in all future calibrations.

We can distill the information in Tables V and VI into a final Table VII which indicates the total variation in T_c observed for all specimens of a given material in SRM units 1, 2, 3, 7, 8, 9, 10, 11 and the expected reproducibility of the T_c of a given specimen. We see, for example, that the T_c of a tungsten sample will fall within ±0.8 mK of 15.9 mK and that its reproducibility might be as good as 0.12 mK and as poor as 0.5 mK. We estimate that the uncertainty in measurement of the resistance can lead to a variation of ±50 μK which could account for the lower limit in the last column of Table VII. The evidence suggests that the upper limit is not due to lack of reproducibility of the GERT itself. The most likely cause of the large standard deviation for some samples is lack of uniformity of the magnetic field in the inner shield. Using the information in the third-to-last column in Table IV, we can calculate that a ±1 μT variation in the remanent magnetic field from experiment to experiment almost exactly gives the largest standard deviation observed for all materials in Table VII. Unfortunately, the magnetic field was not measured so this must remain as a conjecture. At any rate, the user can expect a reproducibility at the worst of ±0.2 mK for the five transitions given by SRM 768 and possibly some improvement if greater care is exercised in reducing the ambient magnetic field. The information contained in Table VII was used as the basis for the entries given in Table I.

TABLE VII

Variation in T_c Observed for SRM 768 Units 1,2,3,7,8,9,10,11

Material	Lowest T_c Observed for a Given Material	Highest T_c	Range	Variation of the standard deviation
	(mK)	(mK)	(mK)	(mK)
W	15.1	17.1	2.0	0.00 - 0.45
Be	21.3	4.8	3.5	0.03 - 0.86
Ir	98.4	99.5	1.1	0.02 - 0.15
$AuAl_2$	160.2	161.0	0.8	0.02 - 0.25
$AuIn_2$	204.9	207.7	2.8	0.13 - 0.25

VI. CONCLUSION

We have described how five superconducting materials were incorporated into a device which can be used with a simple room-temperature detection circuit to define five reference temperatures from 0.015 to 0.206 K. If proper electronic detection techniques are used and care is exercised in reducing the dc magnetic field, the user can expect to obtain a temperature reproducibility of the transitions to no worse than ±0.2 mK.

VII. ACKNOWLEDGMENTS

Many people have made significant contributions to this project which has culminated in SRM 768. A collaboration with Dr. H. Marshak resulted in the intercomparison of the noise and nuclear orientation thermometers which forms the foundation for the temperature scale borne by SRM 768. Dr. D. B. Utton initiated the exploration which led to the selection of $AuA\ell_2$ for the device; he also studied the magnetic properties (magnetization and $H_c(T)$) of $AuA\ell_2$ and $AuIn_2$. Dr. J. F. Schooley offered several suggestions which were incorporated into the device and this document. Mr. F. S. Biancaniello developed the necessary sample preparation techniques and then produced the boules of $AuA\ell_2$ and $AuIn_2$. We thank Mr. L. K. Ives for generously allowing us to use his spark-cutting machine, and Mr. C. H. Brady for making microphotographs of the gold-compound materials. Mr. R. S. Kaeser developed and built several electronic circuits which were of great assistance, and his advice on several experimental matters proved consistently valuable. Mr. S. E. King assisted in many phases of the experimental program (especially in data reduction and analysis) for two summers during the course of this program. Finally, we gratefully acknowledge both the financial support and encouragement from our colleagues in the Office of Standard Reference Materials: Mr. R. K. Kirby, Mr. R. E. Michaelis, and Mr. G. A. Uriano.

Several individuals were generous enough to lend us test samples of many materials. In general, the effect of their loans was to assist us in defining the metallurgical qualities necessary to obtain boules with the desired superconducting properties. Arranged by the material they were kind enough to send, they are:

Be

1. D. L. McElroy, Oak Ridge National Laboratory, Oak Ridge, Tenn.
2. R. L. Falge, Jr., NBS.
3. W. A. Reed, Bell Laboratories, Murray Hill, NJ.
4. G. J. London, The Franklyn Institute Research Laboratories, Philadelphia, PA.

Ir

1. E. Zysk, Englehard Laboratories, Newark, NJ.
2. S. Hornfeldt, Uppsala University, Uppsala, Sweden.
3. D. U. Gubser, U.S. Naval Research Laboratory, Washington, D.C.
4. J. Rexer, Union Carbide Corporation, Parma, Ohio.

$AuAl_2$

1. L. Bennett, NBS.

$AuIn_2$

1. K. Andres, Bell Laboratories, Murray Hill, NJ.

VIII. REFERENCES

[1] To be published, Metrologia.

[2] Schooley, J. F., Soulen, R. J., and Evans, G. A., NBS Special Publication 260-44, U. S. Government Printing Office, Washington, D. C. 20402 (Catalog No. C13.10: 260-44).

[3] Hartshorn, L., J. Sci. Instru. 2, 145 (1924).

[4] Soulen, R. J., Schooley, J. F., and Evans, G. A., Review Sci. Instru. 44, 1537 (1973).

[5] Wheatley, J., Physics 1, 342 (1965).

[6] Gorter, C. J., and Casimir, H. G. B., Phys. Z. 35, 963 (1934); Z. Tech. Phys. 15, 539 (1934).

[7] Bardeen, J., Cooper, L. N., and Schrieffer, J. R., Phys. Rev. 108, 1175 (1957).

[8] Ginsburg, V. L., and Landau, L. D., Zh. Eksperim. i. Teor. Fig. 20, 1064 (1950).

[9] Goodman, B. B., IBM J. Res. Develop. 6, 63 (1962).

[10] Pierce, J., J. Appl. Phys. 44, 1342 (1973); see also, Pierce, J., PhD Thesis, Stanford University.